

New insights into hidden microbiota landscape of *Salvia persepolitana*: evidence of host-specific endophytic fungal communities through a molecular survey

Haniyeh Rashedi¹ · Ali Ganjeali¹ · Javad Asili² · Zahra Tazick² · Abolfaz Shakeri²

Received: 8 June 2025 / Accepted: 27 October 2025 © The Author(s), under exclusive licence to Springer Nature B.V. 2025

Abstract

This study investigated the endophytic fungal diversity associated with Salvia persepolitana, a medicinal plant endemic to Iran. Plant specimens were collected from Khuzestan province of Iran. Taxonomically verified using morphological keys and herbarium comparisons. Endophytic fungi were isolated from root and lower stem tissues. A total of 35 fungal isolates were obtained, with a majority (74%) derived from root tissues. Fungal genomic DNA was extracted, and internal transcribed spacer and large subunit rRNA regions were amplified and sequenced for molecular identification. Sequence analysis revealed dominance of Ascomycota (97.14%), particularly within the Dothideomycetes and Sordariomycetes classes; Pleosporales and Hypocreales orders; Pleosporaceae and Nectriaceae families. The most common genera were Fusarium (40%) and Alternaria (37.14%). Phylogenetic analysis based on the Maximum Likelihood approach identified a total of 21 distinct fungal species. Among these, Alternaria alstroemeriae and Alternaria angustiovoidea were the only taxa recovered from both root and aerial tissues, suggesting a degree of tissue specificity among the endophytic community. Root tissues harbored greater fungal diversity relative to aerial parts, highlighting differential colonization patterns. The dataset encompasses both previously recognized and novel fungal associations, thereby substantially advancing current knowledge of endophytic interactions within the genus Salvia. Except for Fusarium avenaceum, Fusarium redolens, and Phoma herbarum, the remaining 18 taxa represent new records for the genus. Moreover, several species including Fusarium hostae, Alternaria conjuncta, Alternaria malorum, Cladosporium cucumerinum, Diaporthe ambiguea, and Xenodidymella camporesii are reported here, to the best of our knowledge, for the first time as endophytes in any plant host.

Keywords Plant-microbe interaction · Mycobiome · Lamiaceae · Middle east

1 Introduction

Endophytic fungi are intracellular microorganisms that reside symbiotically within plant tissues without causing discernible harm to their host (Omomowo et al. 2023). Extensive investigations have revealed that nearly all vascular and medicinal plant species harbor diverse endophytic communities (Gao et al. 2025). Throughout their lifecycle,

endophytes colonize plant tissues and interact with a variety of environmental microorganisms, including pathogens, rhizosphere bacteria, mycorrhizal fungi, and other endophytes (Omomowo et al. 2023). These interactions can trigger intricate biochemical networks, ultimately leading to the biosynthesis and accumulation of secondary metabolites(Gao et al. 2025). The symbiotic relationships between endophytic fungi and medicinal plants confer mutual benefits: while the plant supplies nutrients to the endophytes, the fungi enhance the plant's metabolic pathways and biosynthetic capabilities (Adeleke and Babalola 2021). Furthermore, endophytes may acquire genetic material that enables them to synthesize bioactive compounds analogous to those produced by their host plants (Gao et al. 2025). Beyond metabolic enhancement, endophytes contribute significantly to plant health by promoting tolerance to abiotic stresses such as

Published online: 11 November 2025



Department of Biology, Faculty of Science, Ferdowsi University of Mashhad, Mashhad, Iran

Department of Pharmacognosy, School of pharmacy, Mashhad University of Medical Sciences, Mashhad, Iran

heavy metals, drought, and salinity, increasing resistance to herbivores and nematodes, and inducing systemic resistance to pathogens (Omomowo et al. 2023).

Salvia persepolitana, represents a plant of particular medicinal interest (Askari et al. 2021). Among the 57 Salvia species identified in Iran, 17 are endemic, with S. persepolitana being exclusively distributed across the provinces of Khuzestan, Isfahan, Ilam, and Shiraz (Asgarpanah 2021). The roots of various Salvia species have been found to contain structurally diverse diterpenoids, predominantly featuring abietane-type carbon skeletons with biological activities (Jassbi et al. 2016). Labdane-type diterpenoids have demonstrated significant pharmacological potential, particularly in anticancer and antimicrobial contexts (Fronza et al. 2011; Jassbi et al. 2016). These bioactive constituents are believed to be, at least in part influenced by its associated endophytic fungi (Gao et al. 2025). Although identifying these root endophytes is the first step in addressing this hypothesis, significant gaps remain regarding their diversity, tissue specificity, and geographic distribution in Salvia species, particularly S. persepolitana (Zimowska et al. 2020). Addressing this knowledge gap, the present study

seeks to isolate, identify, and investigate the communities of endophytic fungi associated within roots of *S. persepolitana*. We also evaluate the differences in endophytic fungal communities in the herbaceous axis tissue originating from the root system above the soil, aiming to identify key root fungal endophytes.

2 Materials and methods

2.1 Collection and taxonomic verification of plant specimens

Healthy and asymptomatic plant specimens, exhibiting no signs of biotic or abiotic stress, were obtained from three distinct regions in Iran: Eslamabad Dowreh (33°37'28.4"N 47°52'48.8"E), Dimeh Darb (31°37'02.1"N 49°29'37.9"E), and Tang-e Māgher (31°00'21.0"N 50°06'38.3"E) at the flowering stage (Fig. 1I-J). To maintain aseptic conditions during collection, plants were carefully excavated using a sterile spade treated with 75% ethanol. Residual soil attached to the root systems was gently dislodged by

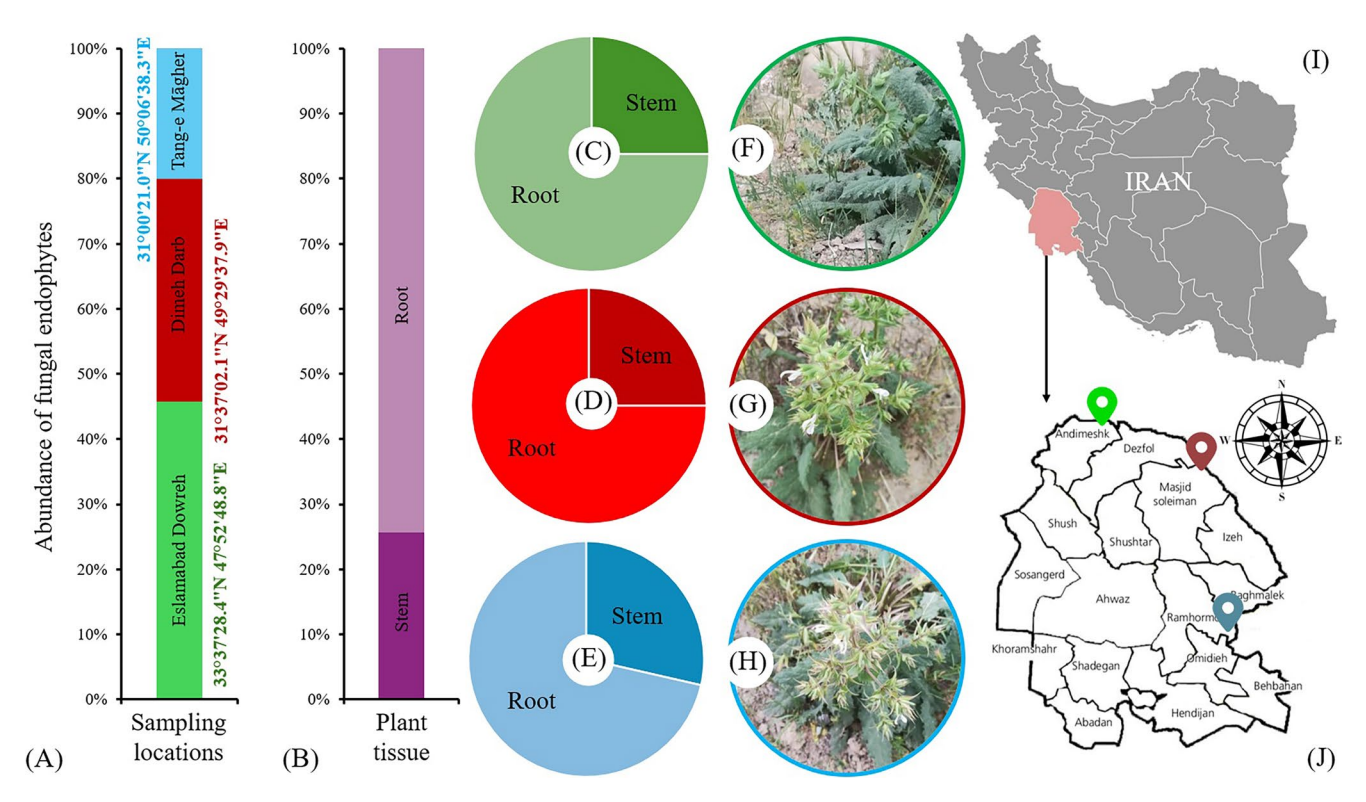


Fig. 1 Geographic origin and tissue-based distribution of endophytic fungi isolated from *Salvia persepolitana*. (A): Frequency of endophytic fungi isolated from each plant sampling location. (B): Frequency of endophytic fungi isolated from different host plant tissues. (C): Tissue-specific distribution of endophytic fungi from the Eslamabad Dowreh sampling site. (D): Tissue-specific distribution of endophytic fungi from the Dimeh Darb sampling site. (E): Tissue-specific distribution

of endophytic fungi from the Tang-e Māgher sampling site. (F): Representative Salsola persepolitana plant sampled from the Eslamabad Dowreh site. (G): Representative Salsola persepolitana plant sampled from the Dimeh Darb site. (H): Representative Salsola persepolitana plant sampled from the Tang-e Māgher site. (I, J): Geographical location of Khuzestan Province within Iran and detailed locations of the sampling sites



minimal agitation to preserve root integrity. Each specimen was promptly enclosed in sterile plastic bags and transported on ice to the laboratory for subsequent analysis. A total of 30 specimens were collected, with 10 plants sampled from each region, to ensure adequate representation of morphological variability. Taxonomic identification at the species level was initially conducted via morphological examination in accordance with the Flora of Iran, No. 76 (Jamzad 2012). To validate the morphological assessments, specimens were further compared with authenticated voucher samples maintained in the herbarium of Mashhad University of Medical Sciences. For broader taxonomic confirmation, diagnostic characteristics were also evaluated against the dichotomous key for Salvia species across Asia (Turdiboev et al. 2022). Following identification, the plant materials were subjected to standard herbarium preparation procedures, including pressing and drying, and were subsequently accessioned into the herbarium collection of Mashhad University of Medical Sciences, each assigned a unique catalog number for future reference.

2.2 Endophytic fungal isolation from plant tissues

Endophytic fungi were isolated from the herbaceous axis originating from the root system (representing the basal segment of the shoot approximately 5 cm above the soil surface), and root tissues of the collected plant specimens. From each of the 30 plants, one segment of basal stem tissue and one segment of root tissue were excised, yielding a total of 20 tissue samples per region (10 stem and 10 root) and 60 tissue samples overall. All samples were subjected to a standardized surface-sterilization protocol, beginning with immersion in 70% ethanol for 1 min, followed by three successive rinses in sterile distilled water. Root tissues received an additional sterilization step involving treatment with 2.5% sodium hypochlorite solution containing Tween-20 for five minutes, succeeded by five successive rinses in sterile distilled water to eliminate residual disinfectant and surfactant, thereby ensuring comprehensive surface sterilization. To assess the effectiveness of the sterilization protocol, control tests were performed by placing sterilized, unsectioned root fragments onto potato dextrose agar (PDA) medium without disturbing internal tissues (Hatamzadeh et al. 2023). Moreover, 100 µL aliquots of the final rinse water were cultured on PDA plates to detect potential microbial contaminants (Akbari Oghaz et al. 2024). Post-sterilization, plant tissues were aseptically cut into approximately 0.5 × 0.5 cm segments using a sterile scalpel and transferred onto PDA supplemented with streptomycin (100 µg/mL) to suppress bacterial growth. Inoculated plates were incubated at 25 ± 2 °C for 1 to 2 weeks, during which fungal outgrowths were monitored. Emergent colonies were isolated and transferred onto fresh PDA plates to obtain axenic cultures for further analysis.

2.3 Crude DNA extraction from fungal isolates

Fungal isolates were cultivated on PDA medium under dark conditions and incubated at 25±2 °C for a period of six days, in accordance with the methodology outlined by Hatamzadeh et al. (2024). For buffer preparation, 1 mL of 1 M 2-Amino-2-(hydroxymethyl)-propane-1,3-diol, 200 μL of 0.5 M ethylenediaminetetraacetic acid (EDTA), 100 µL of 0.1 M sodium chloride, and 50 µL of glycerol were dissolved in 100 mL of double-distilled water, with the solution adjusted to pH 8. To harvest young mycelium (approximately 72 h post-inoculation), sterile toothpicks were employed to gently transfer surface mycelial material from PDA cultures into 1.5 mL microcentrifuge tubes containing 100 µL of the prepared buffer. Samples were vortexed for one minute at 112 m/s², followed by a heat shock treatment at 83±2 °C in a water bath for 35 min. Immediately thereafter, samples were exposed to cold shock by freezing at -20 °C for 15 min. Subsequently, the tubes were centrifuged at 11,200 m/s² for six minutes at 25 ± 2 °C. From each tube, 50 µL of the resulting supernatant was collected and retained as a source of crude fungal DNA for downstream applications.

2.4 Genomic DNA amplification and sequencebased fungal identification

Amplification of the Internal Transcribed Spacer (ITS) and Large Subunit (LSU) ribosomal RNA gene regions was carried out using the polymerase chain reaction (PCR) technique. For ITS region amplification, primer pair ITS5 (5'-G GAAGTAAAAGTCGTAACAAGG-3') and ITS4 (5'-TCC TCCGCTTATTGATATGC-3') was utilized, as outlined by Schoch et al. (2012). The LSU region was similarly amplified using primers LROR (5'-CCCGCTGAACTTAAG C-3') and LR5 (5'-TCCTGAGGGAAACTTCG-3'), following the study of Liu et al. (2012). The PCR reactions were set up in 12.5 μL volumes containing 1× PCR buffer, 10–20 ng of genomic DNA, 0.7 µL of 99.9% dimethyl sulfoxide (DMSO), 0.5 μM of each primer, 25 μM of each dNTP, 2 mM MgCl₂, and 1.0 U of Taq DNA polymerase (NEB). Reactions were performed using a GeneAmp PCR System 9600 (Perkin Elmer, USA) under the following thermocycling parameters: an initial denaturation at 95 °C for 1 min, followed by 40 cycles consisting of denaturation at 95 °C for 30 s, primer annealing at 58 °C for 1 min, and extension at 72 °C for 10 s, applied uniformly to both ITS and LSU targets (Eslami et al. 2025). Resulting amplicons were subjected to sequence analysis via BLASTN against



the NCBI database for initial identification, and corresponding taxonomic classifications were confirmed using the MycoBank database.

2.5 Construction of phylogenetic trees and analysis of evolutionary patterns

Phylogenetic relationships and the evolutionary trajectory of the fungal isolates were reconstructed using the Maximum Likelihood (ML) approach, implemented under the Tamura-Nei nucleotide substitution model. Preliminary tree topologies were generated using the Neighbor-Joining and BioNJ methods, with the topology yielding the highest loglikelihood score selected for final interpretation. The resulting phylogenetic tree was scaled to reflect evolutionary distances, with branch lengths representing the number of substitutions per nucleotide site and illustrating taxonomic clustering. Sequence alignment was carried out prior to ML analysis. The robustness of the phylogenetic inferences was assessed through bootstrap resampling with 1000 replicates. Model selection confirmed the Tamura-Nei model as the most appropriate fit for the dataset, based on the assumption of uniform substitution rates across sites and inclusion of all positions. The heuristic search for the optimal ML tree employed the Nearest-Neighbor Interchange (NNI) algorithm without the application of branch swap constraints. All phylogenetic analyses were conducted using the MEGA12 software, and resulting branch lengths reliably represented the inferred evolutionary divergence.

3 Results

3.1 General morphological description, quantitative morphometric, and taxonomic confirmation

The collected plant species were identified as herbaceous perennials, exhibiting a fragrant aroma and possessing quadrangular, pubescent stems. The foliage appeared dense, with opposite, light green leaves that were thick and exhibited a prominent network of veins, particularly noticeable on the abaxial (lower) surface of the leaf blades. The lower stem leaves were recorded as ovate, measuring 4–5 cm in length, with sharply pointed apices. Leaf margins displayed regular dentition and were attached by petioles. In contrast, the upper stem leaves were noted to be smaller and sessile. The flowers were observed to be white in all sampling locations (Fig. 1F-H). The morphological measurements reported below represent the mean ranges obtained from 10 individuals per site. The plant height varied notably among regions, ranging from 22.23 cm to 38.9 cm, while stem diameter was

observed within a narrower range of 1.63 mm to 2.75 mm. Leaf length and width demonstrated considerable variation, ranging from 18.4 mm to 30.7 mm and 9.6 mm to 19.2 mm, respectively.

The leaf length-to-width ratio fluctuated between 1.5 and 2.1, indicating moderate morphological diversity. Petiole length was recorded in the range of 13.8 mm to 22.7 mm. Inflorescence length ranged from 7.0 cm to 11.1 cm, while node diameter exhibited less variation, measured between 8.0 mm and 11.2 mm. The bract characteristics also showed regional differences, with bract length spanning 9.0 mm to 13.2 mm and bract width from 8.4 mm to 12.3 mm. The bract length-to-width ratio remained relatively stable across regions, with values from 1.0 to 1.4. Corolla length measurements ranged from 12.9 mm to 17.6 mm, and internode distance varied from 9.8 mm to 13.8 mm. Finally, terminal shoot length was found to range between 8.2 mm and 11.9 mm. Based on detailed morphological observations and confirmation through established taxonomic identification keys, all collected specimens were authenticated as S. persepolitana. These specimens have been formally documented and deposited in the Medicinal Plant Herbarium of the School of Pharmacy, Mashhad University of Medical Sciences, under the voucher number 13217.

3.2 Distribution patterns of endophytic fungi across tissues and locations

A total of 35 endophytic fungal isolates were obtained from *S. persepolitana*, with colonization detected in both stem (26%) and root (74%) tissues (Fig. 1B). The distribution of isolates varied among the three sampling locations (Fig. 1A). The Eslamabad Dowreh region yielded the highest number of endophytes (n=16), with 25% isolated from stem tissues and 75% from root tissues. The Dimeh Darb region yielded a moderate number of isolates (n=12), comprising three stem-derived and nine root-derived endophytes. In contrast, the Tang-e Māgher region produced the lowest number of isolates (n=7), with 21% originating from the stem and 71% from the root.

The taxonomic analysis of the isolated endophytic fungi revealed a diverse distribution across multiple hierarchical levels (Fig. 2). At the phylum level, Ascomycota was overwhelmingly dominant, representing 97.14% of the total isolates, whereas Basidiomycota accounted for only 2.85%. Within the class level, four fungal classes were identified. Dothideomycetes and Sordariomycetes constituted the majority, comprising 51.42% and 42.85% of the isolates, respectively. Eurotiomycetes and Agaricomycetes were minimally represented, each with a relative abundance of 2.85%. At the order level, six distinct fungal orders were



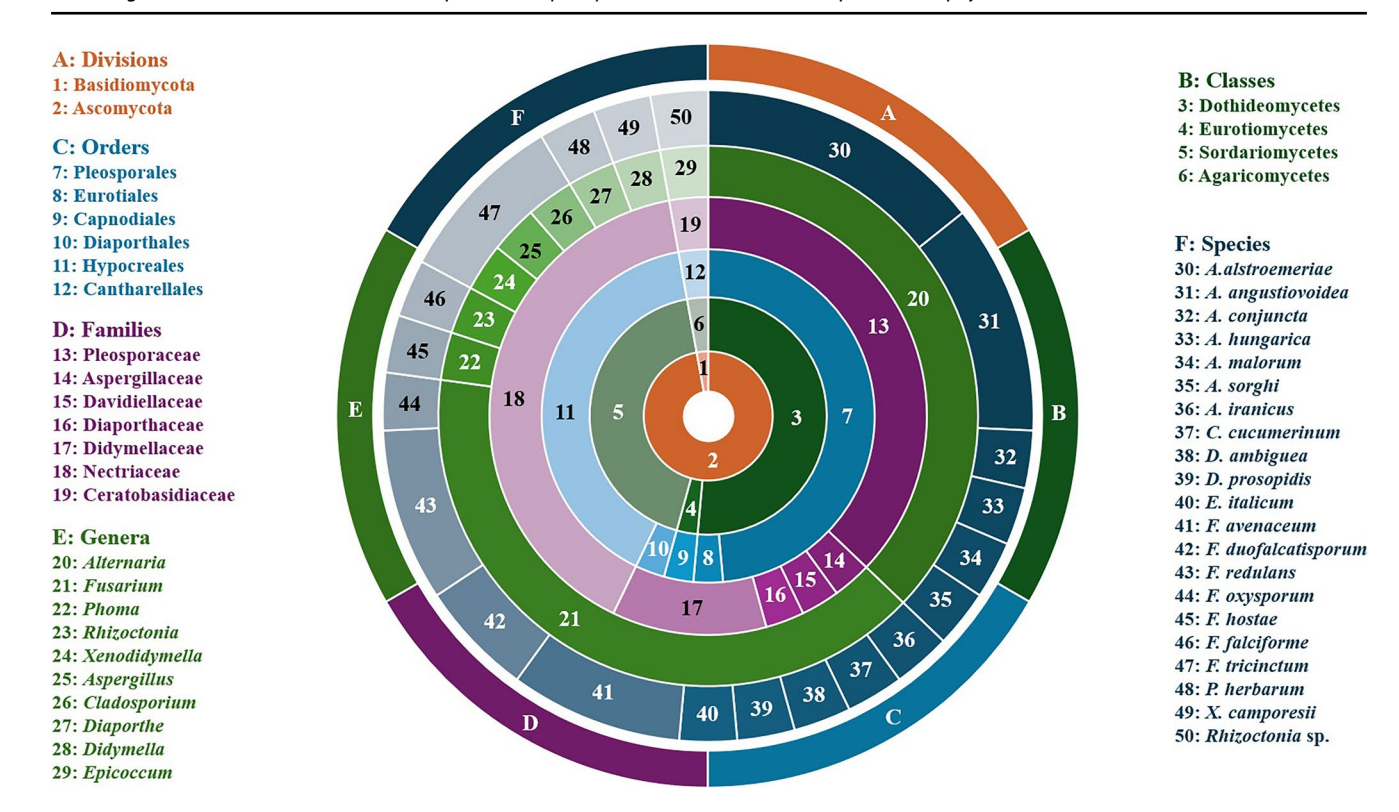


Fig. 2 Taxonomic hierarchy and species composition of endophytic fungi isolated from *Salvia persepolitana*. The concentric rings represent the relative abundance (%) of endophytic fungi across taxonomic

levels. The sectors are scaled by abundance and are not aligned phylogenetically across circles

detected. Pleosporales (48.57%) and Hypocreales (40%) were the most prevalent, indicating their dominant role in the endophytic communities of S. persepolitana. The remaining orders Eurotiales, Capnodiales, Diaporthales, and Cantharellales were each represented by a single isolate (2.85%). The family-level distribution included seven families, with Nectriaceae (40%), Pleosporaceae (37.14%), and Didymellaceae (11.42%) encompassing the highest number of isolates. In contrast, Aspergillaceae, Davidiellaceae, Diaporthaceae, and Ceratobasidiaceae each accounted for only one isolate. Finally, ten fungal genera were identified. Among these, Fusarium (40%) and Alternaria (37.14%) were the most frequently isolated genera. The remaining genera Phoma, Rhizoctonia, Xenodidymella, Aspergillus, Cladosporium, Diaporthe, Didymella, and Epicoccum were each represented by a single isolate, indicating their limited presence within the endophytic fungal community of S. persepolitana.

3.3 Host tissue specificity and relative abundance of identified endophytic fungal species

As illustrated in Figs. 2 and 3 and detailed in Table 1, a total of 21 distinct endophytic fungal species were identified

from S. persepolitana, isolated from both stem and root tissues. Among these, Alternaria alstroemeriae and Alternaria angustiovoidea were the most prevalent, accounting for 14.28% and 11.42% of the total isolates, respectively. These were followed by Fusarium avenaceum (8.57%), Fusarium duofalcatisporum (5.71%), Fusarium redolens (8.57%), and Fusarium tricinctum (8.57%), which exhibited moderate levels of abundance. The remaining 15 species were each represented by a relative frequency of 2.85%, indicating a broad but uneven species distribution. Analysis of tissuespecific colonization patterns revealed that only A. alstroemeriae and A. angustiovoidea were common to both stem and root tissues, constituting 9.52% of the total fungal community, while the remaining 90.47% of species displayed a clear preference for a specific tissue type. In stem tissues, six fungal species were detected, with *Alternaria* spp. dominating the assemblage at 88.88%, and Xenodidymella camporesii being the only non-Alternaria species, with an abundance of 11.1%. Conversely, the root tissue harbored a more diverse fungal community, comprising 26 isolates. Within this compartment, Fusarium spp. were the most prevalent, accounting for 53.84% of the root-associated isolates, while *Alternaria* spp. also exhibited notable representation, comprising 19.23% of the community.



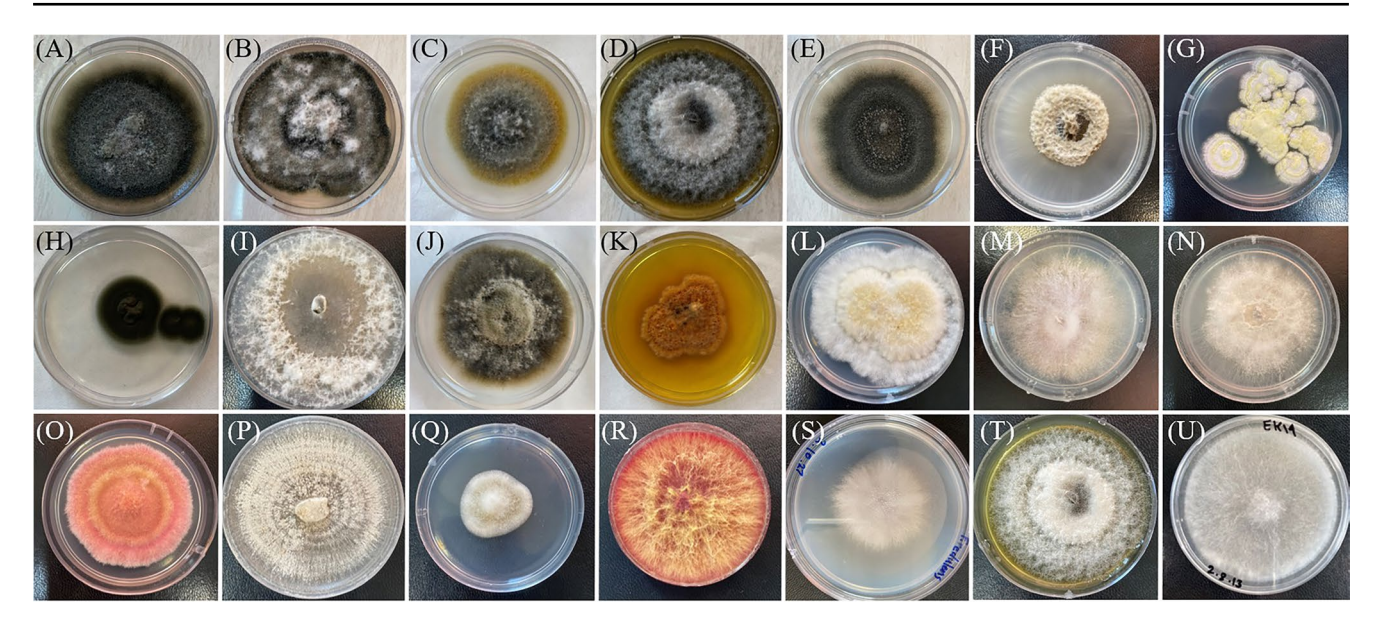


Fig. 3 Colony of endophytic fungal species isolated from Salvia persepolitana grown on PDA after 7 days at 25 ± 2 °C. (A): Alternaria alstroemeriae. (B): Alternaria angustiovoidea. (C): Alternaria conjuncta. (D): Alternaria hungarica. (E): Alternaria Sorghi. (F): Alternaria malorum. (G): Aspergillus iranicus. (H): Cladosporium cucumerinum.

(I): Diaporthe ambiguae. (J): Didymella prosopidis. (K): Epicoccum italicum. (L): Fusarium duofalcatisporum. (M): Fusarium hostae. (N): Fusarium oxysporum. (O): Fusarium tricinctum. (P): Rhizoctonia sp. (Q): Xenodidymella camporesii. (R): Fusarium avenaceum. (S): Fusarium redulans. (T): Phoma herbarum. (U): Fusarium falciforme

3.4 Molecular phylogenetic delineation based on ITS and LSU sequence data

All endophytic fungal species examined in this study were sequenced using standard genomic regions (ITS and LSU). Figure 4 illustrates the phylogenetic relationships of the isolates excluding Alternaria and Fusarium. In Fig. 4A, based on ITS sequences, Epicoccum italicum forms the top clade (Fig. 4-AI), where isolate R21 clusters within the E. italicum clade together with reference isolates, supported by moderate bootstrap values (78-85%), confirming its species identity. The Didymella prosopidis clade (Fig. 4-AII) includes root isolate RE10 clustering with reference isolates with strong support (bootstrap=91%), validating their close phylogenetic placement. In the *Phoma herbarum* clade (Fig. 4A-III), root isolate RE4 groups with reference isolates (bootstrap=68%), supporting its assignment to this species. A distinct pattern is observed in the X. camporesii clade (Fig. 4A-IV), where two reference isolates (MFLUCC 17–2309) and the stem isolate SE8 form a highly supported group (bootstrap=99%). The Diaporthe clade (identified as Diaporthe ambiguea based on LSU data) contains root isolate R26 within a moderately supported branch (bootstrap=58%), indicating affiliation with this species (Fig. 4A-V). In the Aspergillus iranicus clade (Fig. 4A-VI), root isolate RB6 forms a well-supported branch (bootstrap=100%), confirming its identification within this species. The Cladosporium cucumerinum clade (Fig. 4A-VII) places root isolate RB5 together with reference isolates with strong support (bootstrap values=100% and 58%), validating species-level placement. At the base of the tree, isolates of an unidentified *Rhizoctonia* species serve as outgroups (Fig. 4A-VIII), encompassing both basidiomycetous and ascomycetous representatives. Isolate RE12 falls within this group, clustering with a reference strain, confirming its classification as *Rhizoctonia* sp.

Figure 4B presents the phylogenetic relationships of the endophytic fungal isolates based on the LSU genomic region. At the top of the tree, the A. iranicus clade includes root isolate RB6 clustering with reference isolates (bootstrap=96%), confirming its species-level identity. Directly below, the C. cucumerinum clade contains root isolate RB5 grouped with reference isolate CBS 171.52 (bootstrap=65%), validating its taxonomic placement. In the X. camporesii clade, two reference isolates (MFLUCC 17–2309 and A4-3) and the stem isolate SE8 form a strongly supported monophyletic group, confirming their close relatedness at the species level. The E. italicum clade shows root isolate R21 clustering with reference isolates (bootstrap = 92%), supporting its placement within this species. In both the P. herbarum and D. prosopidis clades, the respective root isolates (RE4 and RE10) group with references in closely aligned branches, indicating high genetic similarity and confirming species-level identification. At the base of the tree, the *Rhizoctonia* sp. clade, serving as the outgroup, includes root isolate RE12 clustering with reference isolate 296-17 (bootstrap=83%), validating its placement within this genus.



Table 1 List of endophytic fungal species isolated from different plant tissues of *Salvia persepolitana* with taxonomic classification and Genbank accession number details

Endophytic fungal species	*MUMS P voucher code	Plant tissue	Sampling-location of the host plant	**NCBI accession numbers		ITS fragments (bp)	LSU fragments (bp)
				LSU genomic region	ITS genomic region		
Alternaria alstroemeriae	SE3	Stem	Eslamabad Dowreh	OR008903.1	OR149873.1	525	548
A. alstroemeriae	RE7	Root	Eslamabad Dowreh	OR008904.1	OR149874.1	529	542
A. alstroemeriae	SR2	Stem	Dimeh Darb	OR008926.1	OR149896.1	531	548
A. alstroemeriae	SR10	Stem	Dimeh Darb	OR008927.1	OR149897.1	534	549
A. alstroemeriae	RR10	Root	Dimeh Darb	OR008928.1	OR149898.1	528	545
A. angustiovoidea	SE2	Stem	Eslamabad Dowreh	OR008905.1	OR149875.1	560	529
A. angustiovoidea	RE11	Root	Eslamabad Dowreh	OR008906.1	OR149876.1	561	528
A. angustiovoidea	RE14	Root	Eslamabad Dowreh	OR008907.1	OR149877.1	566	529
A. angustiovoidea	SR1	Stem	Dimeh Darb	OR008929.1	OR149899.1	562	528
A. conjuncta	RE2	Root	Eslamabad Dowreh	OR008908.1	OR149878.1	582	576
A. hungarica	SE1	Stem	Eslamabad Dowreh	OR008909.1	OR149879.1	527	574
A. malorum	SB4	Stem	Tang-e Māgher	OR008919.1	OR149889.1	595	840
A. sorghi	SB5	Stem	Tang-e Māgher	OR008920.1	OR149890.1	553	605
Aspergillus iranicus	RB6	Root	Tang-e Māgher	OR008921.1	OR149891.1	596	809
Cladosporium cucumerinum	RB5	Root	Tang-e Māgher	OR008922.1	OR149892.1	551	864
Diaporthe ambiguea	R26	Root	Dimeh Darb	OR008930.1	NS***	528	
Didymella prosopidis	RE10	Root	Eslamabad Dowreh	OR008910.1	OR149880.1	535	584
Epicoccum italicum	R21	Root	Dimeh Darb	OR008931.1	OR149900.1	526	832
Fusarium avenaceum	RB4	Root	Tang-e Māgher	OR008923.1	OR149893.1	523	720
F. avenaceum	RE4	Root	Eslamabad Dowreh	OR008911.1	OR149881.1	522	586
F. avenaceum	RR3	Root	Dimeh Darb	OR008932.1	OR149901.1	521	720
F. duofalcatisporum	RE5	Root	Eslamabad Dowreh	OR008912.1	OR149882.1	544	849
F. duofalcatisporum	RE6	Root	Eslamabad Dowreh	OR008913.1	OR149883.1	542	845
F. redulans	RE9	Root	Eslamabad Dowreh	OR008914.1	OR149884.1	559	867
F. redulans	RE15	Root	Eslamabad Dowreh	OR008915.1	OR149885.1	560	859
F. redulans	RR5	Root	Dimeh Darb	OR008935.1	OR149905.1	558	845
F. oxysporum	RB7	Root	Tang-e Mägher	OR008924.1	OR149894.1	542	865
F. hostae	RR4	Root	Dimeh Darb	OR008933.1	OR149902.1	553	870
F. falciforme	RR7	Root	Dimeh Darb	OR015784.1	OR149906.1	569	810
F. tricinctum	RB2	Root	Tang-e Māgher	OR008925.1	OR149895.1	562	848
F. tricinctum	RR11	Root	Dimeh Darb	OR008934.1	OR149903.1	560	850
F. tricinctum	RR15	Root	Dimeh Darb	OR008936.1	OR149904.1	557	850
Phoma herbarum	RE4	Root	Eslamabad Dowreh	OR008916.1	OR149886	544	881
Rhizoctonia sp.	RE12	Root	Eslamabad Dowreh	OR008917.1	OR149887.1	719	851
Xenodidymella camporesii	SE8	Stem	Eslamabad Dowreh	OR008917.1	OR149888.1	542	830

^{(*):} Microbial culture collection of Mashhad University of Medical Sciences. (**): National Center for Biotechnology Information. (***): Not sequenced

3.4.1 Phylogenetic structure of Alternaria species

The ITS-based phylogenetic analysis classified *Alternaria* isolates into six distinct clades (Fig. 5A). At the top of the tree, the *Alternaria conjuncta* clade (Fig. 5A-I) comprises four isolates, including root isolate RE2, which forms an independent branch with strong bootstrap support (100%), confirming its placement within the *A. conjuncta* clade. Similarly, in the *Alternaria malorum* clade (Fig. 5A-II), stem isolate SB4 appears on a strongly supported branch

(bootstrap=100%), supporting its identification as *A. malorum*. In the *Alternaria hungarica* clade (Fig. 5A-III), stem isolate SE1 forms a distinct branch (bootstrap=94%), validating its assignment to this species. The *Alternaria sorghi* clade (Fig. 5A-IV) includes stem isolate SB5 on an individual branch (bootstrap=86%), supporting species-level identification. The two largest clades *A. angustiovoidea* and *A. alstroemeriae* demonstrate more complex internal structures. In the *A. angustiovoidea* clade (Fig. 5A-V), root isolates RE11 and RE14 cluster together (bootstrap=49%),



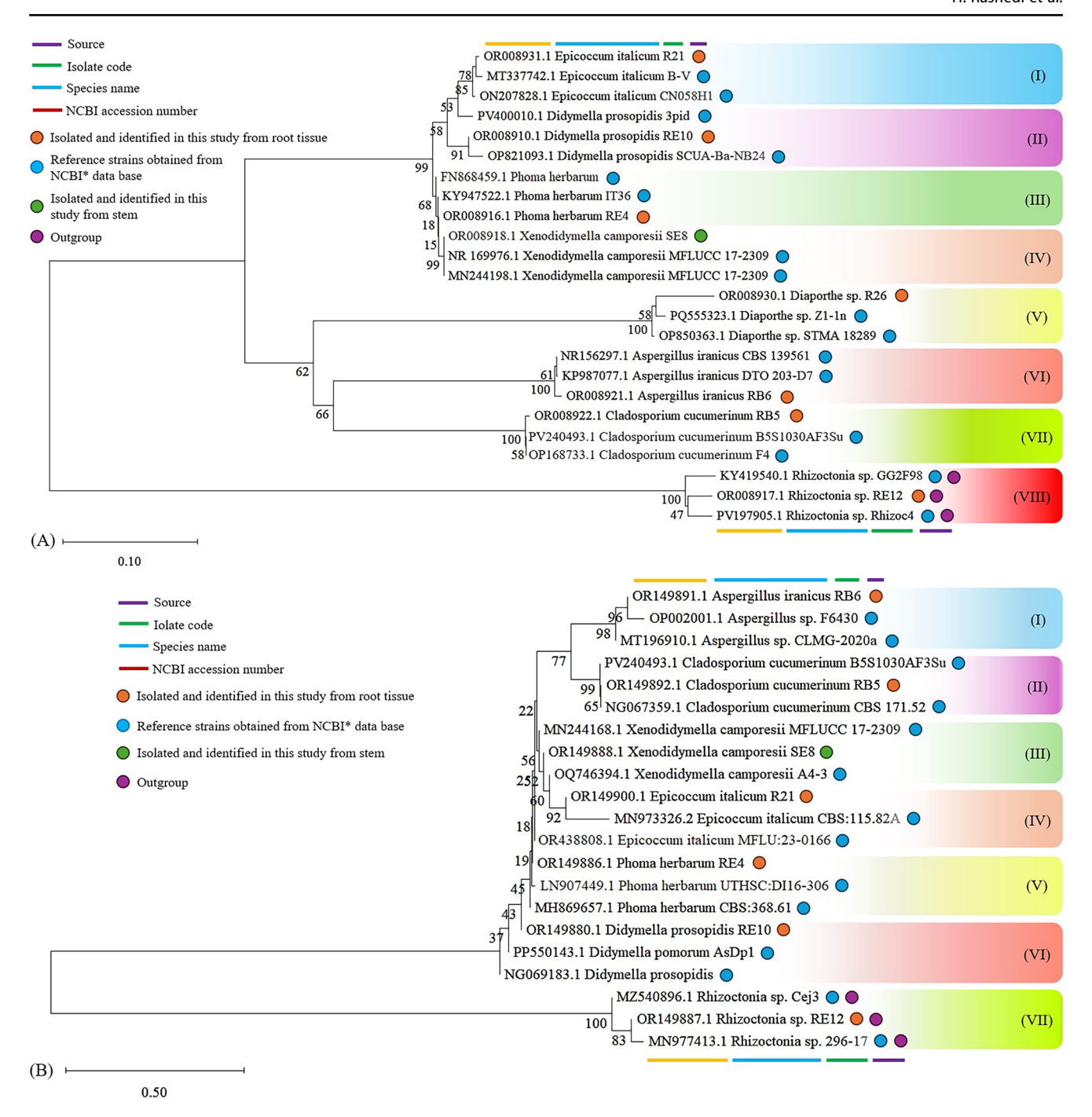


Fig. 4 Phylogenetic analysis and evolutionary insights into endophytic fungi associated with *Salvia persepolitana*. (A): A phylogenetic tree generated using sequences from the internal transcribed spacer (ITS) region, incorporating 24 nucleotide sequences and covering 901

while stem isolate SE2 and SR1 occupy neighboring branches, collectively supporting their classification within this species despite weak internal resolution. At the bottom of the tree, the *A. alstroemeriae* clade (Fig. 5A-VI) includes three single-branch isolates (SR10, SR2, and RR10), all positioned within the species clade along with reference isolates, confirming their identity as *A. alstroemeriae*. Root

aligned positions in the final dataset. (**B**): A phylogenetic tree based on the large subunit (LSU) rRNA region, constructed from 21 nucleotide sequences with a total alignment length of 1,738 positions. All bifurcations are shown in Supplementary Fig. S1

isolate RE7 clusters with reference isolate WZ-879 (bootstrap=83%), further validating its placement in this species clade.

Phylogenetic analysis of *Alternaria* species using the LSU region reveals moderate to low bootstrap support across several clades, reflecting varying levels of genetic convergence (Fig. 5B). At the top of the tree, the *A. conjuncta* clade



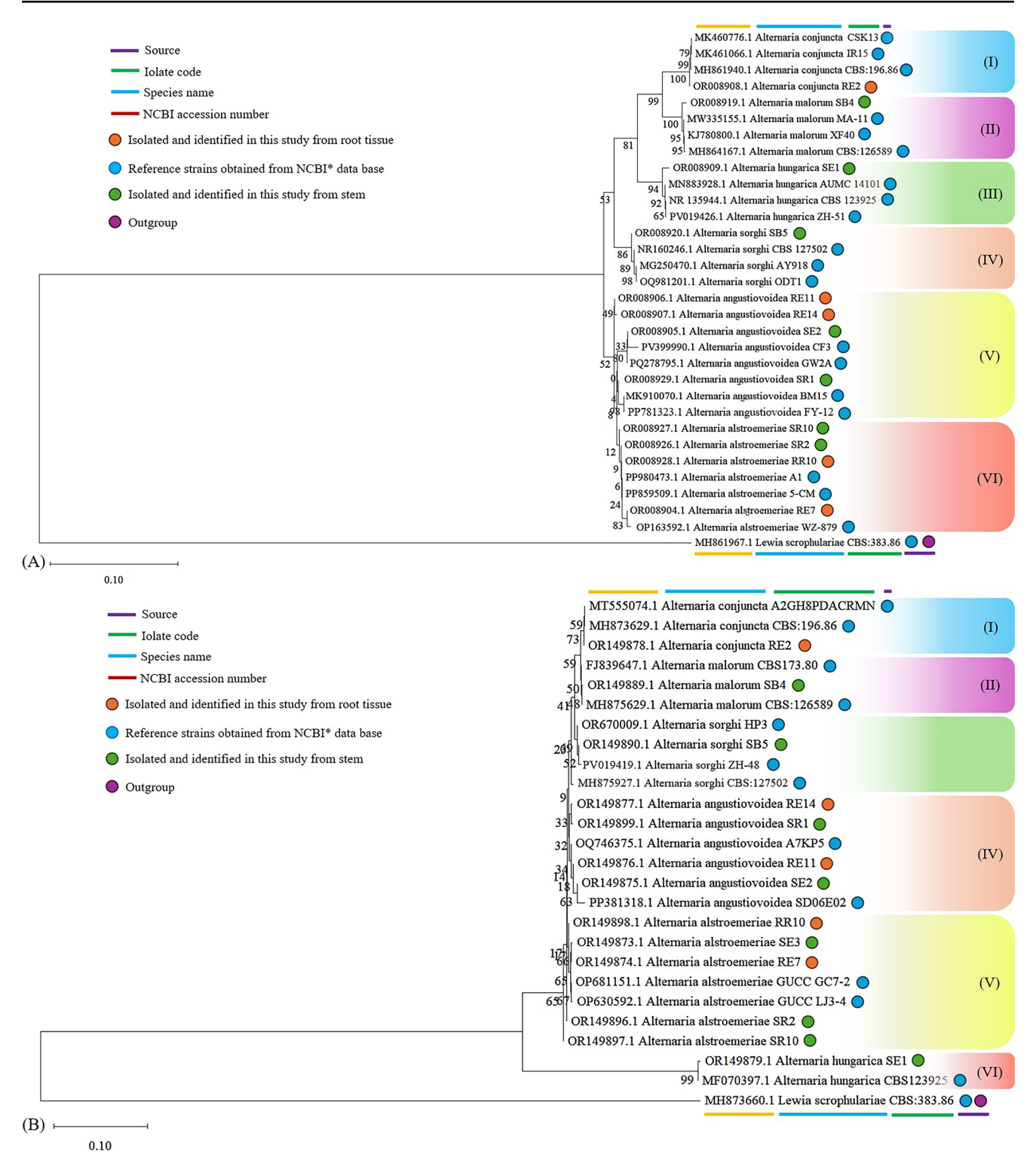


Fig. 5 Phylogenetic reconstruction and evolutionary characterization of *Alternaria* endophytic fungi isolated from *Salvia persepolitana*. (A): Maximum likelihood phylogenetic tree inferred from internal transcribed spacer (ITS) region sequences, comprising 32 fungal isolates and aligned across 881 nucleotide positions. (B): Phylogenetic

tree constructed using sequences from the large subunit (LSU) rRNA region, including 26 isolates with a total alignment length of 1006 nucleotide positions. The complete resolution of bifurcations is provided in Supplementary Fig. S2



(Fig. 5B-I) includes root isolate RE2, which is positioned on an individual branch (bootstrap = 73%) within the broader A. conjuncta clade, confirming its taxonomic placement. Further down, the A. malorum clade (Fig. 5B-II) places stem isolate SB4 within a weakly supported subcluster (bootstrap=50%), nevertheless consistent with its identification as A. malorum. In the A. sorghi clade (Fig. 5B-III), stem isolate SB5 clusters within the clade with moderate bootstrap support (52%), reinforcing species-level assignment. The A. angustiovoidea clade (Fig. 5B-IV) exhibits a more complex topology. Stem isolate SR1 and root isolate RE14 appear in weakly supported subclusters (bootstrap=33%), together with neighboring references, indicating ambiguous but consistent placement within the species clade. Stem isolate SE2 groups with reference isolate SD06E02 (bootstrap=63%), further supporting species-level identification. In the A. alstroemeriae clade (Fig. 5B-V), most isolates from this study occupy distinct branches, consistent with their placement within this species. Stem isolate SE3 and root isolate RE7 form a moderately supported subcluster (bootstrap=66%), aligning with reference isolates that cluster separately (bootstrap=65%). Remaining isolates also fall within the clade, reinforcing species-level identification. The A. hungarica clade (Fig. 5B-VI) comprises stem isolate SE1 together with the reference strain CBS 123,925 in a strongly supported subcluster (bootstrap = 99%), confirming its placement within this species.

3.4.2 Phylogenetic resolution of *Fusarium* species

The ITS-based phylogenetic analysis delineates several Fusarium species clades with varying degrees of bootstrap support (Fig. 6A). At the top of the tree, the F. duofalcatisporum clade (Fig. 6A-I) includes two root isolates (RE6 and RE5), which form a strongly supported subcluster (bootstrap=93%), confirming their placement within this species. In the Fusarium oxysporum clade (Fig. 6A-II), root isolate RB7 is positioned on an individual branch (bootstrap=94%), supporting its classification as F. oxysporum. The Fusarium falciforme clade (Fig. 6A-III) consists of root isolate RR7 and reference DTO 422-H8 forming a strongly supported group (bootstrap=99%), validating specieslevel identity. The F. redolens clade (Fig. 6A-IV) includes three root isolates (RE15, RE9, and RR5), each occupying separate branches but consistently assigned to this species together with references. In the Fusarium hostae clade (Fig. 6A-V), root isolate RR4 groups within the clade, albeit with weak support (bootstrap=34%), suggesting tentative placement. The F. avenaceum clade (Fig. 6A-VI) contains root isolates RR3, RB4, and RE4, all positioned on separate branches, but supported within the species clade along with multiple references. The F. tricinctum clade (Fig. 6A-VII) includes root isolates RR15, RR11, and RB2, which cluster with reference isolates, confirming species-level affiliation.

The LSU-based phylogenetic tree (Fig. 6B) provides robust resolution of Fusarium species associations. At the top, the F. avenaceum clade (Fig. 6B-I) includes root isolate RB4 on an individual branch (bootstrap=72), while RE4 and RR3 cluster together (bootstrap=72%), all falling within the species clade alongside references. In the F. tricinctum clade (Fig. 6B-II), root isolates (RR11, RR15, RB2) and reference strains form a highly supported cluster (bootstrap=99%), demonstrating strong taxonomic cohesion. Similarly, in the F. hostae clade (Fig. 6B-III), root isolate RR4 groups with references with moderate support (bootstrap=80%), confirming species placement. Within the F. redolens clade (Fig. 6B-IV), isolates RR5, RE15, and RE9 occupy separate but supported branches (bootstrap=66–97%), consistently positioned within the species. The F. oxysporum clade (Fig. 6B-V) consists of root isolate RB7 and references in a weakly supported subcluster (bootstrap=53%), nevertheless indicating assignment to this species. In the F. duofalcatisporum clade (Fig. 6B-VI), root isolates RE5 and RE6 cluster together with references, confirming their taxonomic placement. At the base of the tree, the F. falciforme clade (Fig. 6B-VII) includes root isolate RR7 and a reference strain forming a well-supported subcluster (bootstrap=79%), validating its species-level identity.

4 Discussion

The morphological variation observed among populations of S. persepolitana appears to reflect ecological differences between sites rather than plant age, as all specimens were sampled at the flowering stage. Plants from cooler, higher-latitude sites tended to be shorter with smaller leaves, while those from warmer regions showed comparatively larger dimensions, consistent with known phenotypic plasticity in Salvia species (Turdiboev et al. 2022). Our investigation revealed the coexistence of 21 fungal species as endophytes within S. persepolitana. To date, there are no prior reports documenting the endophytic fungal diversity in S. persepolitana, highlighting the novelty of our findings. Nevertheless, several of the identified taxa correspond to genera or species previously reported as endophytes in other Salvia species, thereby corroborating their endophytic potential within the genus. In line with our findings, A. iranicus has previously been reported as an endophyte of *Houttuynia cordata* (Rao et al. 2024). In particular, Salvia aegyptiaca leaves from Gebel Elba, Egypt, have yielded multiple Aspergillus



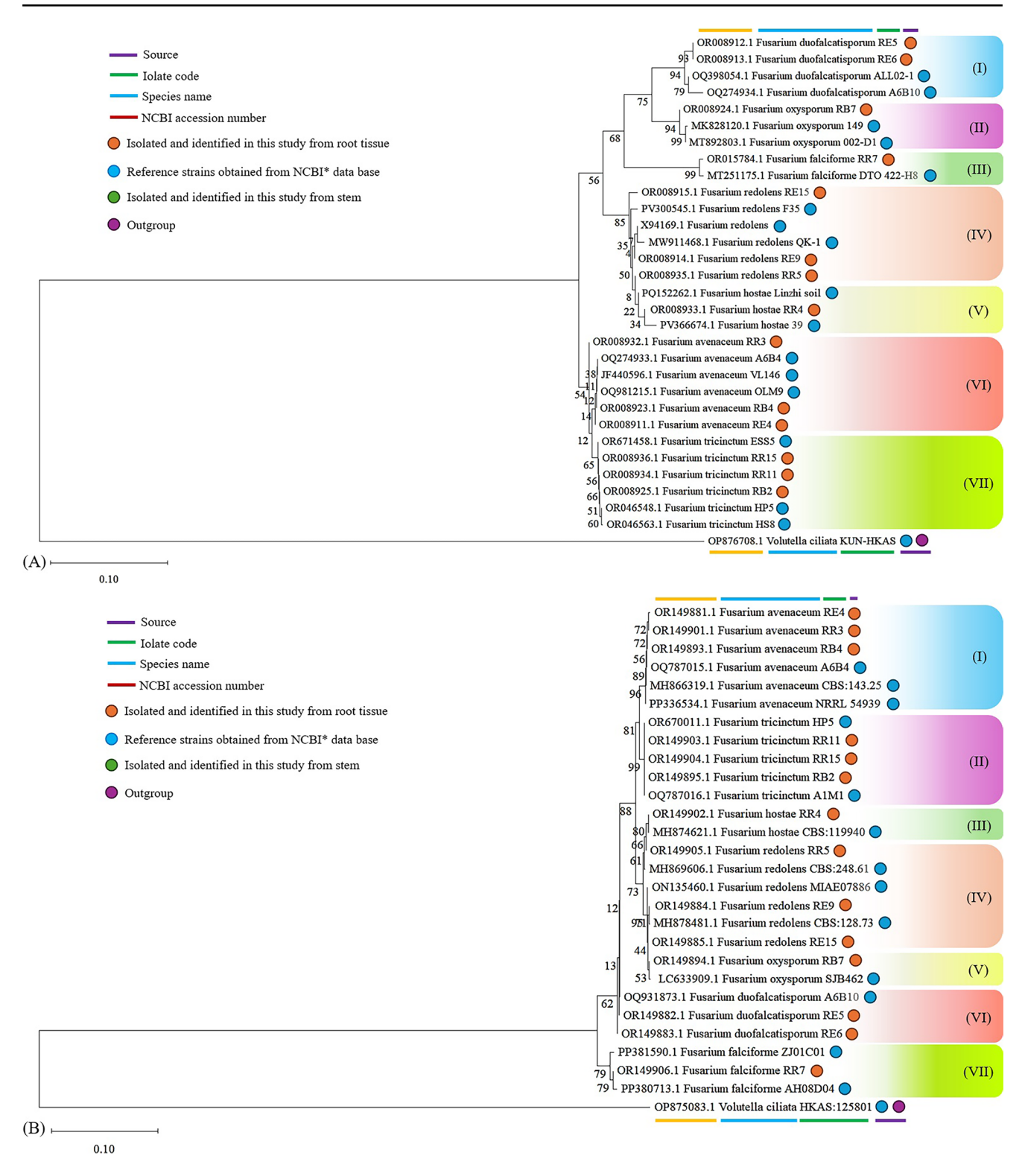


Fig. 6 Phylogenetic inference and evolutionary assessment of *Fusarium* endophytic fungi associated with *Salvia persepolitana*. (A): Phylogenetic tree generated via maximum likelihood analysis based on internal transcribed spacer (ITS) region sequences, incorporating 31

isolates with 1547 aligned nucleotide positions. (**B**): Tree derived from large subunit (LSU) rRNA region sequences, constructed using 28 fungal isolates and a total sequence alignment of 946 positions. Details of all bifurcations are available in Supplementary Fig. S3



species, including Aspergillus brasiliensis, Aspergillus nidulans, Aspergillus niger, and Aspergillus terreus (El-Bondkly et al. 2020). Aspergillus foeniculicola was isolated from the root of Salvia miltiorrhiza in Shaanxi, China (Ma et al. 2011), while an unidentified Aspergillus sp. was reported from S. miltiorrhiza roots in Beijing, China (Lou JingFeng et al. 2013), and from Salvia abrotanoides leaves in Zoshk, Iran (Teimoori-Boghsani et al. 2020). While the current literature does not establish an endophytic association for C. cucumerinum in plants making this the first report of such a relationship only a limited number of species within the genus Cladosporium have previously been documented in association with the genus Salvia. Notably, Cladosporium cladosporioides has been reported from the leaves of S. aegyptiaca in the Gebel Elba region of Egypt (El-Bondkly et al. 2020). Although D. ambigua has not previously been documented as an endophyte, several unidentified species of the *Diaporthe* genus have been isolated from plant tissues. Specifically, endophytic Diaporthe spp. have been reported from the stems of S. miltiorrhiza in Sichuan, China (Li et al. 2015), as well as from the stems of S. abrotanoides and Salvia yangii in Wroclaw, Poland (Zimowska et al. 2020).

In alignment with our findings, D. prosopidis has been previously documented as an endophyte in apple (Liu et al. 2023). Additionally, several species within the genus including Didymella pedeiae and Didymella glomerata, have been reported as endophytes in the roots and leaves of S. miltiorrhiza in China (Li et al. 2016; Lou JingFeng et al. 2013). Consistent with our observations, E. italicum has been reported as an endophyte in the leaf tissue of wheat in the Giza Governorate, Egypt (Rashad et al. 2025). Furthermore, a literature review identified Epicoccum sorghinum as an endophytic species associated with S. miltiorrhiza (Wang et al. 2025). Consistent with our observation of an unidentified Rhizoctonia species as an endophyte of S. persepolitana, a study by Wang et al. (2021) confirmed the endophytic association of *Rhizocto*nia bataticola with S. miltiorrhiza. In this study, we report X. camporesii as an endophyte; however, neither this species nor other congeners within the genus Xenodidymella have previously been documented in association with Salvia species. Furthermore, to the best of our knowledge, no reports exist regarding endophytic relationships involving this species with any other plant hosts. Additionally, P. herbarum D603, as reported by Chen et al. (2020), is known to colonize root tissues and establish a stable symbiotic relationship with its host plant S. miltiorrhiza. Another species of this genus Phoma glomerata D14 has also reported as an endophytic fungus from S. miltiorrhiza (Li et al. 2016).

4.1 Diversity and novelty of endophytic *Fusarium* species

Two species warrant specific attention due to their documented endophytic presence in related contexts. F. oxysporum was among twenty fungal species from fourteen genera isolated as leaf endophytes of S. aegyptiaca collected from Gebel Elba (El-Bondkly et al. 2020). This species has also been reported in association with the roots and stems of Salvia multicaulis across its native range in Iran, including the provinces of Qazvin, Alborz, and Mazandaran (Jahromi et al. 2021). Furthermore, F. redolens has been found in the root of S. miltiorrhiza in Beijing, China (Lou JingFeng et al. 2013). In addition to F. oxysporum and F. redolens, five additional Fusarium species were isolated as endophytes from S. persepolitana in the present study. The endophytic behavior of Fusarium species within Salvia species has been welldocumented, with several species isolated from different plant parts and geographic locations.

Fusarium dlaminii and Fusarium solani were reported from the roots of S. abrotanoides in Darrud, Iran (Teimoori-Boghsani et al. 2020), while Fusarium proliferatum was isolated from the roots of S. miltiorrhiza in both Shandong, China (Li et al. 2015), and Iran (Jahromi et al. 2021). Fusarium asiaticum was also detected in the leaf tissue of S. multicaulis in Iran (Jahromi et al. 2021). Additionally, Fusarium equiseti was previously reported in the hairy roots of S. miltiorrhiza and was also recorded in Wenjiang (Li et al. 2024). It is important to note that the Fusarium species identified in the present study F. avenaceum, F. duofalcatisporum, F. hostae, F. falciforme, and F. tricinctum are distinct from those previously reported in association with Salvia species. However, their endophytic associations with other plant taxa have been documented, thereby supporting the plausibility of our findings. For instance, endophytic relationships involving F. avenaceum, F. duofalcatisporum, and F. tricinctum have been reported in Achillea wilhelmsii and Achillea arabica (Eslami et al. 2025). Additionally, F. falciforme strain R-423 has been isolated as an endophyte from pigeon pea (Cajanus cajan) (Fu et al. 2025). In contrast, no previous reports exist concerning the endophytic behavior of F. hostae, making this the first documented instance of its association with a plant host, to the best of our knowledge.

4.2 Established associations and geographic distribution of endophytic *Alternaria* species

Notably, seven *Alternaria* species were isolated as endophytes. Of these, five have previously been reported as



endophytes in other plant taxa, supporting their potential endophytic capacity. For instance, A. angustiovoidea was identified as a floral endophyte in A. arabica (Eslami et al. 2025), while A. alstroemeriae has been reported in association with Catharanthus roseus (Li et al. 2025). Similarly, A. hungarica has been documented as an endophyte in soybean (Glycine max) by Abdelmagid et al. (2023). Furthermore, endophytic interactions involving other Alternaria species and Urtica dioica (common nettle) have been described by Salmi et al. (2021). Although these findings suggest a potential for broad host adaptability within the genus Alternaria, the existence of such a relationship should not be far-fetched in Salvia species. The endophytic behavior of Alternaria species has been evident in Salvia species to date, with various strains reported from diverse geographic regions and plant organs. Alternaria alternata has been isolated from the leaf of S. aegyptiaca in Gebel Elba, Egypt (El-Bondkly et al. 2020), and from the flower of S. miltiorrhiza in Shandong, China (Li et al. 2015) or Alternaria multiformis from S. multicaulis in Iran (Jahromi et al. 2021). Alternaria chlamydosporigena was found in the root of S. abrotanoides in Zoshk, Iran (Teimoori-Boghsani et al. 2020), and in the root of S. miltiorrhiza in Beijing, China (Lou JingFeng et al. 2013). Additionally, an unspecified Alternaria sp. has been identified in multiple plant parts (root, shoot, and leaf) of S. miltiorrhiza in Henan, China (Zhou et al. 2018); in the leaf and stem of S. abrotanoides; and in S. yangii in Wroclaw, Poland (Zimowska et al. 2020). However, no previous reports were found in the literature documenting the endophytic behavior of A. conjuncta, and A. malorum as identified in the present study. Thus, their endophytic association appears to be novel and reported here for the first time.

5 Conclusion

This study presents the first comprehensive account of endophytic fungal diversity within *S. persepolitana*, uncovering a total of 21 fungal species across multiple genera. The findings reveal both well-established and previously unreported associations, significantly enriching our understanding of endophytic relationships within the genus *Salvia*. With the exception of *F. avenaceum*, *F. redolens*, and *P. herbarum*, all 18 of the identified endophytic fungal species represent novel records for the genus *Salvia*. Notably, several species such as *F. hostae*, *A. conjuncta*, *A. malorum*, *C. cucumerinumand*, *D. ambiguea*, and *X. camporesii* are documented here for the first time as plant-associated endophytes. The detection of numerous *Fusarium* and *Alternaria* species, many of which

have been previously identified in diverse plant taxa and geographic contexts, reflects the ecological adaptability and potential functional roles of these fungi within plant microbiomes. Our findings not only reinforce the genus *Salvia* as a reservoir of endophytic fungal diversity but also highlight the importance of underexplored medicinal plants in discovering novel fungal symbionts. These insights provide a valuable foundation for future studies aimed at understanding the ecological significance, functional roles, and potential biotechnological applications of these endophytes.

Appendix A

The ITS and LSU genome sequences of the endophytic fungi, which identified in this research are available online at Nucleotide database of National Center for Biotechnology Information (htpp://www.ncbi.nlm.nih.gov).

Supplementary Information The online version contains supplementary material available at https://doi.org/10.1007/s13199-025-01094-7.

Acknowledgements This study received financial support from Ferdowsi University of Mashhad, Ministry of Science, Research, and Technology, Iran. We also express our gratitude to the Department of Pharmacognosy, School of pharmacy, Mashhad University of Medical Sciences for facilitating measurements and the analyses in their laboratories.

Author contributions Haniyeh Rashedi: performed the experiments, data analysis, wrote and revised the manuscript. Ali Ganjeali and Javad Asili supervised the whole research work, administrated the project, and revised the manuscript. Zahra Tazick: Methodology, Data curation and writing — original draft. Abolfaz Shakeri: Methodology, Data curation. All authors contributed to the editing and approved the final version of the manuscript.

Funding This work was supported by Ferdowsi University of Mashhad (grant number 3/55827).

Data availability The raw data can be made available upon reasonable request from corresponding author.

Declarations

Ethics approval and consent to participate This article reports no studies involving human participants or animals conducted by any of the authors. All authors have provided their approval to participate in this research and to contribute to the manuscript.

Consent for publication All authors approved this manuscript to be published.

Competing interest The authors declare that they have no known competing financial interests or personal relationships that could have appeared to influence the work reported in this paper.



References

- Abdelmagid A, Hou A, Wijekoon C (2023) Endophytic fungi of soybean (*Glycine max* (L.) Merr.) and their potential applications. Can J Plant Sci 104(1):32–40. https://doi.org/10.1139/cjps-202 3-0070
- Adeleke BS, Babalola OO (2021) Pharmacological potential of fungal endophytes associated with medicinal plants: a review. J Fungi 7(2):147. https://doi.org/10.3390/jof7020147
- Akbari Oghaz N, Rahnama K, Habibi R, Razavi SI, Farias ARG (2024) Endophytic and rhizospheric *Trichoderma* spp. Associated with cucumber plants as potential biocontrol agents of *Fusarium oxys*porum f. sp. cucumerinum. Asian J Mycol 7(1):31–46. https://doi .org/10.5943/ajom/7/1/3
- Asgarpanah J (2021) A review on the essential oil chemical profile of *salvia* genus from Iran. Nat Volatiles Essent Oils 8(3):1–28. https://doi.org/10.37929/nyeo.852794
- Askari SF, Avan R, Tayarani-Najaran Z, Sahebkar A, Eghbali S (2021) Iranian *Salvia* species: a phytochemical and pharmacological update. Phytochemistry 183:112619. https://doi.org/10.1016/j.phytochem.2020.112619
- Chen HM, Wu HX, He XY, Zhang HH, Miao F, Liang ZS (2020) Promoting Tanshinone synthesis of *Salvia miltiorrhiza* root by a seed endophytic fungus, *Phoma herbarum* D603. China J Chin Materia Med 45(1):65–71. https://doi.org/10.19540/j.cnki.cjcmm.20191113.101
- El-Bondkly AAM, El-Gendy MMAA, El-Bondkly EAM, Ahmed AM (2020) Biodiversity and biological activity of the fungal microbiota derived from the medicinal plants *Salvia aegyptiaca* L. and *Balanties aegyptiaca* L. Biocatal Agric Biotechnol 28:101720. ht tps://doi.org/10.1016/j.bcab.2020.101720
- Eslami Z, Tazik Z, Asili J, Soheili V, Akbari Oghaz N, Rezaei T, Mottaghipisheh J, Shakeri A (2025) Unveiling the endophytic fungal communities in Iranian *Achillea* species: molecular insights into host specificity and colonization patterns. Symbiosis 95:225–240. https://doi.org/10.1007/s13199-025-01043-4
- Fronza M, Murillo R, Ślusarczyk S, Adams M, Hamburger M, Heinzmann B, Laufer S, Merfort I (2011) In vitro cytotoxic activity of abietane diterpenes from *Peltodon longipes* as well as *Salvia miltiorrhiza* and *Salvia Sahendica*. Bioorg Med Chem 19(16):4876–4881. https://doi.org/10.1016/j.bmc.2011.06.067
- Fu JX, Jiao J, Gai QY, Gao J, Wang XQ, Zhang ZY, He J, Wen MN, Fu YJ (2025) A novel endophytic fungus Fusarium falciforme R-423 for the control of Rhizoctonia solani root rot in pigeon pea as reflected by the alleviation of reactive oxygen species-mediated host defense responses. J Agric Food Chem 73(6):3373–3388. ht tps://doi.org/10.1021/acs.jafc.4c09886
- Gao Y, Xu Y, Dong Z, Guo Y, Luo J, Wang F, Yan L, Zou X (2025) Endophytic fungal diversity and its interaction mechanism with medicinal plants. Molecules 30(5):1028. https://doi.org/10.3390 /molecules30051028
- Hatamzadeh S, Rahnama K, White JF, Akbari Oghaz N, Nasrollahnejad S, Hemmati K (2023) Investigation of some endophytic fungi from five medicinal plants with growth promoting ability on maize (*Zea Mays* L). J Appl Microbiol 134(1):lxac015. https://doi.org/10.1093/jambio/lxac015
- Hatamzadeh S, Akbari Oghaz N, Rahnama K, Noori F (2024) Combination of a hierarchical and thermal shock process with a specific aqueous buffer: a safe, rapid and reliable DNA extraction method for plant endophytic fungi. Biologia 79(2):597–604. https://doi.org/10.1007/s11756-023-01579-0
- Jahromi MS, Azizi A, Soltani J (2021) Diversity and spatiotemporal distribution of fungal endophytes associated with Salvia multicaulis. Curr Microbiol 78(4):1432–1447. https://doi.org/10.1007 /s00284-021-02430-y

- Jamzad Z (2012) Flora of Iran, No. 76: the family lamiaceae Martinov. Forest and Rangeland Research Institute of Iran, Tehran, Iran
- Jassbi AR, Zare S, Firuzi O, Xiao J (2016) Bioactive phytochemicals from shoots and roots of *Salvia* species. Phytochem Rev 15:829–867. https://doi.org/10.1007/s11101-015-9427-z
- Li YL, Xin XM, Chang ZY, Shi RJ, Miao ZM, Ding J, Hao GP (2015) The endophytic fungi of *Salvia miltiorrhiza* Bge. f. alba are a potential source of natural antioxidants. Bot Stud 56(5):1–7. https://doi.org/10.1186/s40529-015-0086-6
- Li X, Zhai X, Shu Z, Dong R, Ming Q, Qin L, Zheng C (2016) *Phoma glomerata* D14: an endophytic fungus from *Salvia miltiorrhiza* that produces Salvianolic acid C. Curr Microbiol 73:31–37. https://doi.org/10.1007/s00284-016-1023-y
- Li X, Lin Y, Qin Y, Han G, Wang H, Yan Z (2024) Beneficial endophytic fungi improve the yield and quality of *Salvia miltiorrhiza* by performing different ecological functions. PeerJ 12:e16959. ht tps://doi.org/10.7717/peerj.16959
- Li YF, Yue F, Wan XR, Li C, Sun Y, Pei YH (2025) Antimicrobial perylenequinones isolated from the endophytic fungus *Alternaria alstroemeriae*. Phytochem Lett 65:64–67. https://doi.org/10.1016/j.phytol.2024.12.003
- Liu KL, Porras-Alfaro A, Kuske CR, Eichorst SA, Xie G (2012) Accurate, rapid taxonomic classification of fungal large-subunit rRNA genes. Appl Environ Microbiol 78(5):1523–1533. https://doi.org/10.1128/AEM.06826-11
- Liu Jj, Zheng J, Gao C, Liu H, Zhang Dh, Liu L (2023) Screening of endophytic growth-promoting fungi and their characteristics in Apple. J Fruit Sci 40:735–746. https://doi.org/10.13925/j.cnki.g sxb.20220495
- Lou JingFeng LJF, Fu LinYun FLY, Luo RuiYa LRY, Wang XiaoHan WX, Luo HaiYu LHY, Zhou LiGang ZL (2013) Endophytic fungi from medicinal herb Salvia miltiorrhiza bunge and their antimicrobial activity. Afr J Microbiol Res 7(47):5343–5349
- Ma C, Jiang D, Wei X (2011) Mutation breeding of Emericella foeniculicola TR21 for improved production of Tanshinone IIA. Process Biochem 46(10):2059–2063. https://doi.org/10.1016/j.procbio.2011.07.012
- Omomowo IO, Amao JA, Abubakar A, Ogundola AF, Ezediuno LO, Bamigboye CO (2023) A review on the trends of endophytic fungi bioactivities. Sci Afr 32(46):e01594. https://doi.org/10.1186/s41938-022-00547-1
- Rao J, Tao Z, Chen J, Yang S (2024) Investigation of bioactive metabolites produced by the endophytic fungus *Aspergillus Iranicus* from *Houttuynia cordata* thunb. Nat Prod Res 12:1–5. https://doi.org/10.1080/14786419.2024.2412836
- Rashad YM, El-Sharkawy HHA, Abdalla SA, Ibrahim OM, Elazab NT (2025) Unraveling the regulating effect of the endophyte *Epicoccum italicum* HE20 on the biosynthetic genes of polyphenols in wheat in response to yellow rust. Physiol Mol Plant Pathol 138:102705. https://doi.org/10.1016/j.pmpp.2025.102705
- Salmi D, Riou C, Issawi M, Titouche Y, Ambrosini V, Smail-Saadoun N, Abbaci H, Houali K (2021) Antibacterial and antioxidant activities of endophytic fungi and nettle (*Urtica dioica L.*) leaves as their host. Cell Mol Biol 67(3):204–211. https://doi.org/10.14715/cmb/2021.67.3.33
- Schoch CL, Seifert KA, Huhndorf S, Robert V, Spouge JL, Levesque CA, Chen W, Consortium FB, List FBCA, Bolchacova E (2012) Nuclear ribosomal internal transcribed spacer (ITS) region as a universal DNA barcode marker for Fungi. Proc. Natl. Acad. Sci. 109(16):6241–6246. https://doi.org/10.1073/pnas.1117018 109
- Teimoori-Boghsani Y, Ganjeali A, Cernava T, Müller H, Asili J, Berg G (2020) Endophytic fungi of native *Salvia abrotanoides* plants reveal high taxonomic diversity and unique profiles of secondary metabolites. Front Microbiol 10:3013. https://doi.org/10.3389/fmicb.2019.03013



- Turdiboev OA, Shormanova AA, Sheludyakova MB, Akbarov F, Drew BT, Celep F (2022) Synopsis of the central Asian *salvia* species with identification key. Phytotaxa 543(1):1–20. https://doi.org/10.11646/phytotaxa.543.1.1
- Wang GK, Yang JS, Huang YF, Liu JS, Tsai CW, Bau DT, Chang WS (2021) Culture separation, identification and unique anti-pathogenic fungi capacity of endophytic fungi from Gucheng Salvia miltiorrhiza. In Vivo 35(1):325–332. https://doi.org/10.21873/invivo.12263
- Wang Y, Cai S, Tao Z, Peng J, Li D, Li L, Cao X, Jiang J (2025) Isolation of endophytic fungi and effects on secondary metabolites in hairy roots of *Salvia miltiorrhiza*. J Microbiol Biotechnol 9(35):e2411051. https://doi.org/10.4014/jmb.2411.11051
- Zhou LS, Tang K, Guo SX (2018) The plant growth-promoting fungus (PGPF) *Alternaria* sp. A13 markedly enhances *Salvia miltiorrhiza* root growth and active ingredient accumulation under

- greenhouse and field conditions. Int J Mol Sci 19(1):270. https://doi.org/10.3390/ijms19010270
- Zimowska B, Bielecka M, Abramczyk B, Nicoletti R (2020) Bioactive products from endophytic fungi of sages (*Salvia* spp). Agriculture (Basel) 10(11):543. https://doi.org/10.3390/agriculture10110543

Publisher's note Springer Nature remains neutral with regard to jurisdictional claims in published maps and institutional affiliations.

Springer Nature or its licensor (e.g. a society or other partner) holds exclusive rights to this article under a publishing agreement with the author(s) or other rightsholder(s); author self-archiving of the accepted manuscript version of this article is solely governed by the terms of such publishing agreement and applicable law.

